Supporting Information

High Performance Graphene Nanowalls/Si Self-powered Photodetectors with HfO_2 as an Interfacial Layer

Yuheng Shen[a, b], Yulin Li[a, b], Wencheng Chen[a,b], Sijie Jiang[a], and Qijin Cheng[a, b,*]

[a)] School of Electronic Science and Engineering, Xiamen University, Xiamen, 361102, P. R. China.

[b)] Shenzhen Research Institute of Xiamen University, Shenzhen, 518000, P. R. China.

*E-mail: qijin.cheng@xmu.edu.cn

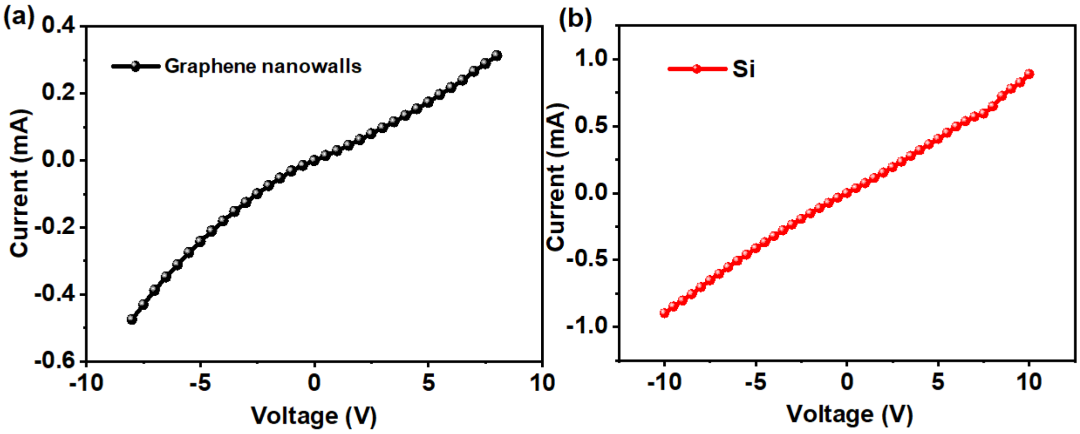

Figure S1. Ohmic contact of **(a)** GNWs and **(b)** Si.

The current-voltage characteristic curves for Cr/Au-GNWs-Cr/Au and Cr/Au-Si-Cr/Au are shown in Figure S1a and S1b, respectively. The almost linear I-V characteristic curves indicate that quasi ohmic contact is formed.

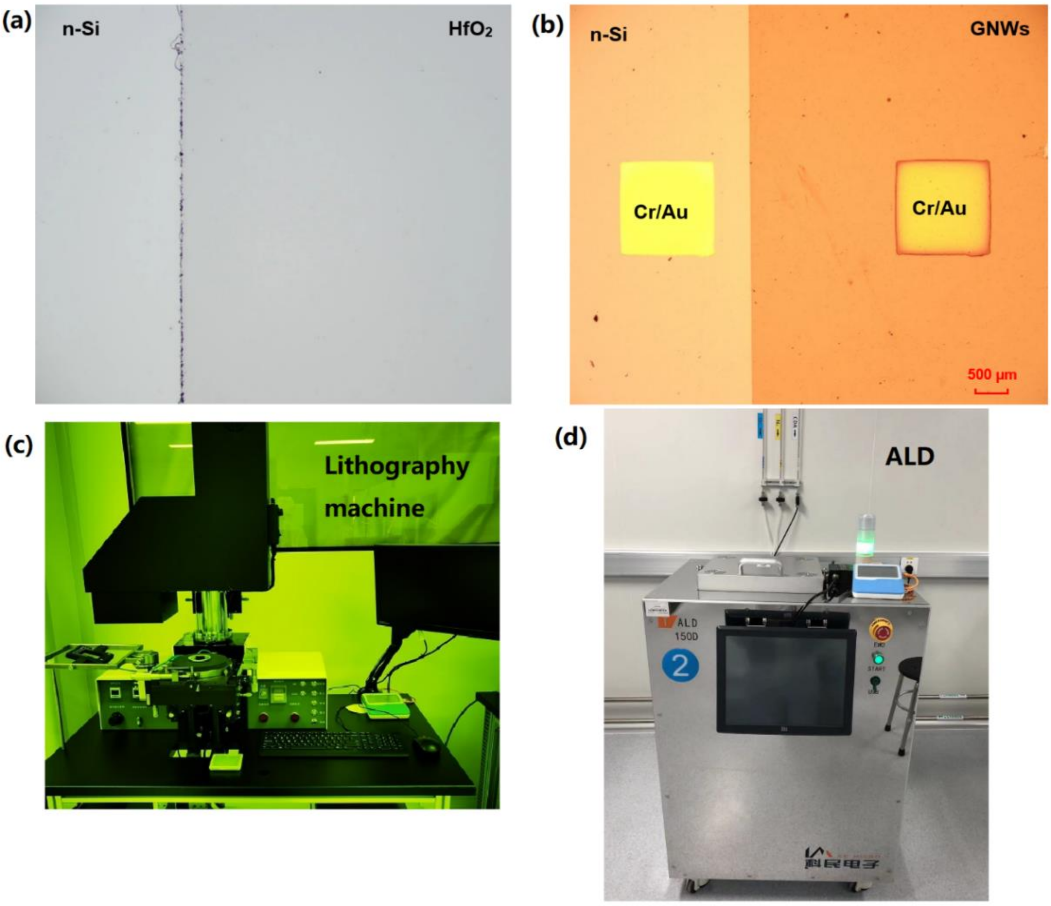

Figure S2. (a) Photograph of the Si substrate with a 3 nm HfO_2 layer (the two-thirds area of the Si substrate was covered with a 3 nm HfO_2 layer). **(b)** Photograph of the GNWs/HfO_2/Si photodetector. **(c)** Photograph of lithography equipment. **(d)** Photograph of ALD equipment.

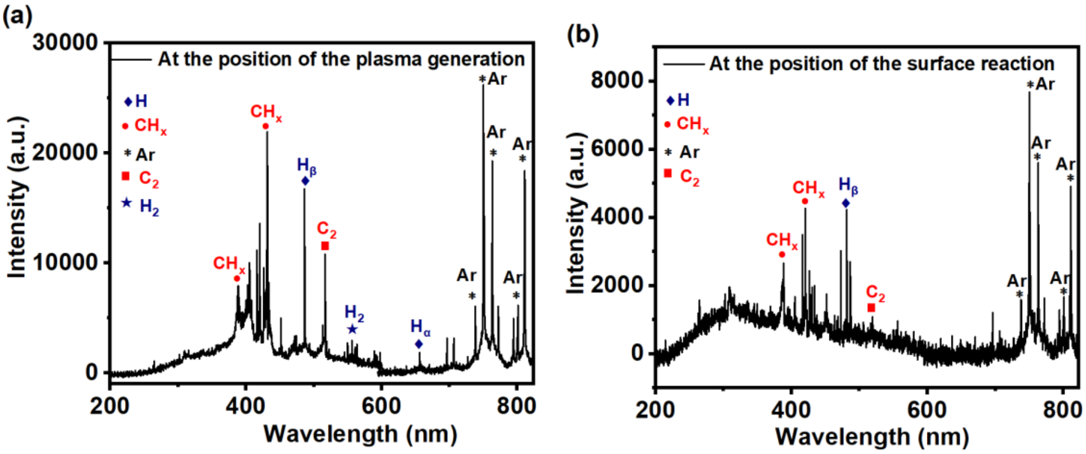

Figure S3. OES spectra at different positions of the remote PECVD system: **(a)** at the position of the plasma generation and **(b)** at the position of the surface reaction.

Figure S3 shows OES spectra at different positions of the remote PECVD system in the growth process of GNWs under the condition of a CH_4/Ar flow rate ratio of 10 sccm/40 sccm, an RF power of 300 W, a growth temperature of 900 °C and a growth time of 120 s. As shown in Figure S3a, a series of spectral lines, including C_2, CH_x, Ar, H_α, H_β, H_2, etc., can be observed at the position of the plasma generation. Notably, Figure S3a exhibits several argon spectral lines with a high intensity, located in the 750-820 nm range. In contrast, Figure S3b does not show the spectra lines of H_α and H_2 at the position of the surface reaction, which is favorable for the decrease of the etching effect by H-related radicals. Moreover, the intensity of argon spectral lines decreases at the position of the surface reaction, which can effectively reduce the impact of the unwanted ion bombardment.

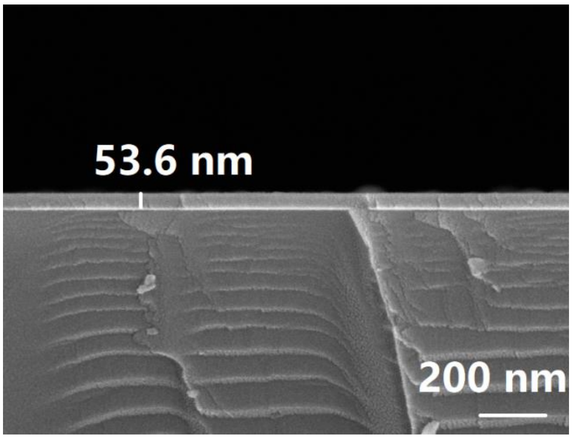

Figure S4. A cross-sectional SEM image of HfO_2 grown on the Si substrate for 500 cycles. As shown in Figure S4, the thickness of HfO_2 is approximately 53.6 nm and the growth rate is calculated to be 1.07 Å/cycle.

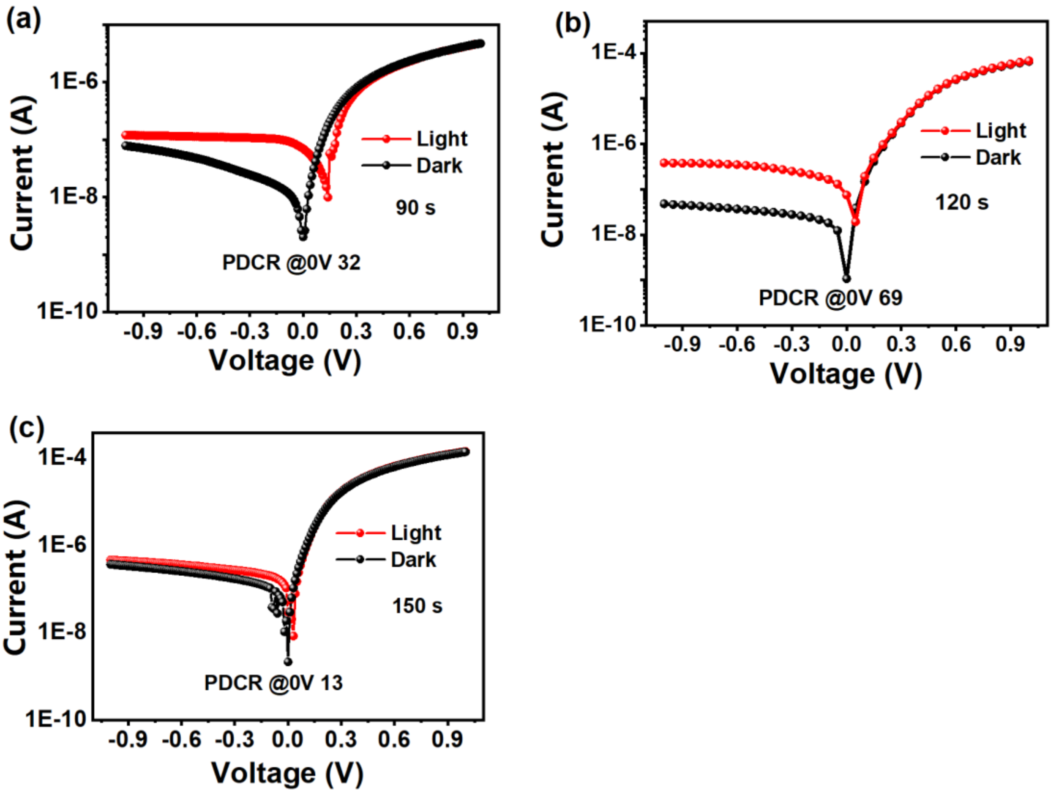

Figure S5. I-V characteristic curves of the GNWs/HfO_2/Si photodetectors with different growth times of GNWs **(a)** 90 s, **(b)** 120 s **(c)** 150 s, respectively.

Figure S5 shows the I-V characteristic curves of the GNWs/HfO_2/Si photodetectors with different growth times of GNWs. Table S1 lists the photoelectric parameters of the GNWs/HfO_2/Si photodetectors with different growth times of GNWs. As shown in Table S1, the photodetector for GNWs grown for 120 s shows the best performance among all the fabricated devices.

Table S1. Photoelectric parameters of the GNWs/HfO_2/Si photodetectors with different growth times of GNWs.

Time (s)	**Current under dark condition (A)**	**Current under light condition (A)**	**PDCR @ 0V**	**Responsivity (A/W)**
90	$2.02 \times 10^{-9}\ A$	$6.91 \times 10^{-8}\ A$	32	0.054
120	$1.07 \times 10^{-9}\ A$	$7.38 \times 10^{-8}\ A$	69	0.058
150	$2.16 \times 10^{-9}\ A$	$2.98 \times 10^{-8}\ A$	13	0.023

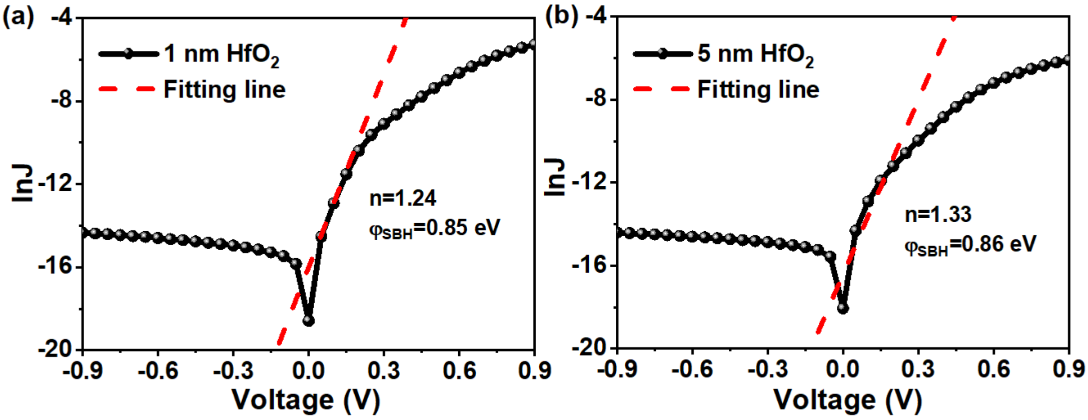

Figure S6. LnJ-V curves of the GNWs/Si photodetectors with the thickness of **(a)** 1 nm, **(b)** 5 nm HfO_2 layer.

Figure S6 shows the lnJ-V curves of the GNWs/Si photodetectors with different thicknesses of HfO_2 interface layer. We can obtain n and φ_{SBH} by fitting the linear part of the curve based on the equations (5) and (6). The results of the barrier height for photodetectors with 1 nm and 5 nm HfO_2 are 0.85 eV and 0.86 eV, respectively. The results of the ideality factor for photodetectors with 1 nm and 5 nm HfO_2 are 1.24 and 1.33, respectively.